

# Coherent Detection Using Optical Time-Domain Sampling

Xin Chen, Xiaobo Xie, *Member, IEEE*, Inwoong Kim, *Member, IEEE*, Guifang Li, *Senior Member, IEEE*, Hanyi Zhang, and Bingkun Zhou

**Abstract**—Coherent optical time-domain sampling is proposed to relax the requirement for photodetector bandwidth as well as the speed of analog-to-digital converter (ADC) and digital signal processing. Transmission of 10-Gb/s binary phase-shift keying signals over 220-km standard single-mode fiber was demonstrated using 10-Gsa/s ADCs.

**Index Terms**—Coherent optical fiber communication, digital signal processing (DSP), dispersion compensation, optical time-domain sampling, phase estimation.

## I. INTRODUCTION

**H**OMODYNE and intradyne coherent detection for optical fiber communication re-emerged recently owing to the development of high-speed digital signal processing (DSP) [1]–[4]. It provides a promising way to improve receiver sensitivity, increase spectral efficiency, enable complicated modulation formats, and utilize electronic postprocessing. In particular, electronic dispersion compensation (EDC) in a coherent-detected system has received significant attention because it is low cost, flexible, and can remove the penalty caused by optical dispersion-compensating modules [1], [2]. The coherent receiver requires very fast analog-to-digital converters (ADCs) with a sampling rate equivalent to the symbol rate to convert the received signal to the digital domain. If EDC needs to be applied, the signal electrical field has to be obtained. With a reasonable and practical signal bandwidth equal to its symbol rate assumed for a nonreturn-to-zero (NRZ) signal, a sampling rate twice the symbol rate is required according to the Nyquist theorem. After ADCs, a DSP unit performs postprocessing, phase estimation, and data recovery. The high processing rate required for ADCs and DSP limits real-time implementation of coherent detection. Parallelization is necessary to relax the requirement for these components and has been employed for carrier recovery [3].

Manuscript received September 24, 2008; revised November 11, 2008. First published January 06, 2009; current version published February 11, 2009. This work was supported in part by Defense Advanced Research Projects Agency (DARPA) under Contract DAAD1702C0097.

X. Chen was with CREOL, University of Central Florida, Orlando, FL 32816 USA and also with the Department of Electronic Engineering, Tsinghua University, Beijing 100084, China (e-mail: chenxin02@gmail.com).

X. B. Xie and G. Li are with CREOL, University of Central Florida, Orlando, FL 32816 USA (e-mail: xiaoboxie@gmail.com; li@creol.ucf.edu).

I. Kim was with CREOL, University of Central Florida, Orlando, FL 32816 USA and is now with Fujitsu Laboratories of America, Inc., Richardson, TX 75082 USA (e-mail: inwoong.kim@us.fujitsu.com).

H. Zhang and B. Zhou are with the Department of Electronic Engineering, Tsinghua University, Beijing 100084, China (e-mail: zhy-dee@tsinghua.edu.cn; zbk-dee@tsinghua.edu.cn).

Digital Object Identifier 10.1109/LPT.2008.2010868

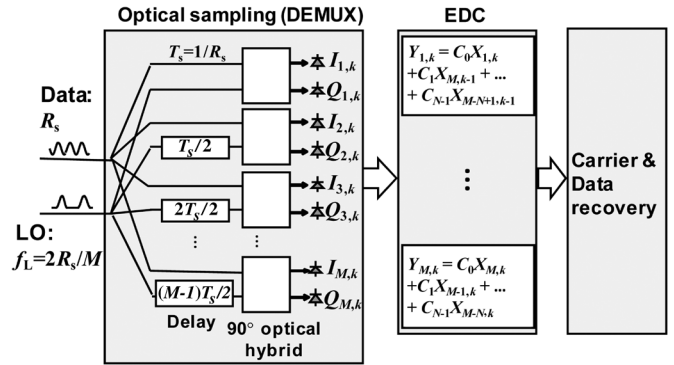


Fig. 1. Configuration of parallel optical sampling and postprocessing.

In this letter, we present coherent optical time-domain sampling (COTDS) and parallel processing configuration for coherent detection and postprocessing to effectively decrease the required photodetector (PD) bandwidth, ADC speed, and DSP rate. Multiple optical pulse trains instead of a continuous-wave (CW) light are used as local oscillators (LOs) and beat with received signal, respectively, so the signal is coherently sampled into several COTDS tributaries. All the tributaries are then detected, digitized, and processed in parallel. Transmission and EDC of the 10-Gb/s binary phase-shifting keying (BPSK) signal over 220-km standard single-mode fiber (SSMF) were demonstrated using 10-Gsa/s ADCs to verify the feasibility of this scheme.

## II. PRINCIPLE OF PARALLEL PROCESSING

Fig. 1 illustrates the configuration of COTDS and the subsequent EDC. Assuming the data is NRZ and has a symbol rate of  $R_s$ , a sampling rate of  $2R_s$  is necessary to recover the useful signal spectrum to perform dispersion compensation. A pulse source with a repetition rate of  $f_L = 2R_s/M$  is divided into  $M$  pulse trains ( $M$  is an integer) and interleaved in the time domain to form the LOs for COTDS. The relative delay between neighboring pulse trains is  $T_s/2 = T_L/M$ , equal to the reduced sampling period, where  $T_s = 1/R_s$  and  $T_L = 1/f_L$ . The received data signal is coupled into  $M$   $90^\circ$  optical hybrids with the COTDS pulse trains. Assuming LO pulses are narrow enough, the complex amplitude of the beat between the signal and the LO in each pulse duration is proportional to the signal field at the LO pulse center. So the signal is optically sampled at  $2R_s/M$  in each tributary, as shown in Fig. 2. The outputs of the hybrids are then photodetected and digitized by ADCs. The PD bandwidth requirement scales with the optical sampling rate. Hence, it can be reduced by a factor of  $M$ . All the ADCs work at  $f_L$ , which is

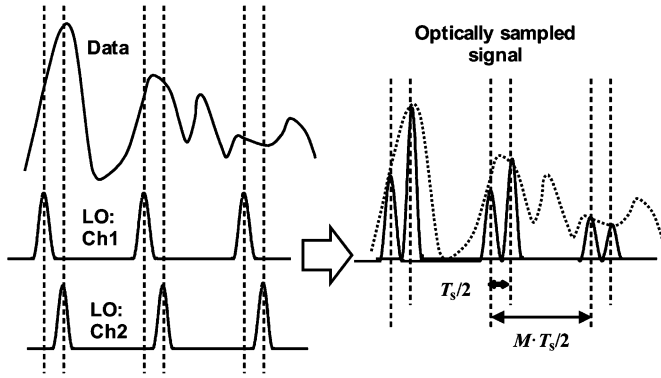


Fig. 2. Principle of COTDS.

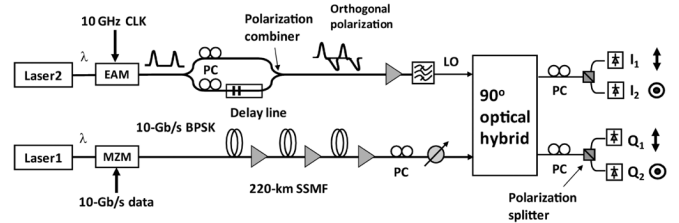
the same as the COTDS pulse repetition rate and could be much lower than the symbol rate. Therefore, the multiple LO pulse trains perform COTDS. Note that electronic demultiplexing can also be employed for each tributary to further parallelize the signal and reduce the processing rate [3]. After the ADCs, multiple COTDS tributaries are available simultaneously and EDC can be performed in parallel using  $M$  finite impulse response (FIR) filters [5]. In Fig. 1,  $X_{i,k} = I_{i,k} + jQ_{i,k}$  is the output of the  $i$ th tributary, where  $k$  is the index in time domain, and  $C_n$  are the coefficients of the FIR filters. The FIR filter can be designed from the impulse response (inverse Fourier transform) of the chromatic dispersion transfer function  $\exp(j(1/2)\omega^2\beta_2L)$ , where  $\omega$  is the angular frequency,  $\beta_2$  is the fiber group velocity dispersion parameter, and  $L$  is the fiber length. Buffers and multiply-accumulate units are needed in each filter. Each filter operates at a speed of  $2R_s/M$ , the same as the speed of the ADCs, while the overall sampling rate is  $2R_s$ . After dispersion compensation, the signal is resampled to one sample per symbol (sampling rate =  $R_s$ ) and phase estimation is performed to recover the data, which can be done in parallel as well [3]. In the entire configuration, each module processes only signals that are already available, so the scheme can be carried out in real time.

The coherence between all the COTDS LO pulse trains can be realized using integrated waveguide configuration with feedback control. However, this puts a significant burden on hardware. Alternatively, hardware phase locking between the COTDS LO pulse trains can be replaced by phase estimation in the software domain, which is more desirable especially for a large number of COTDS tributaries.

### III. EXPERIMENTAL SETUP AND RESULTS

A  $1 \times 2$  COTDS scheme was carried out experimentally to demonstrate 10-Gb/s NRZ BPSK transmission and dispersion compensation. The setup is shown in Fig. 3. A 10-Gb/s BPSK signal after 220-km SSMF ( $D = 17$  ps/(km · nm)) transmission was coherently detected using COTDS and the dispersion was electronically compensated. For dispersion compensation, a sampling rate of 20 Gsa/s is required for 10-Gb/s signal. In our experiment, the sampling rate of ADCs was set at 10-Gsa/s, and two COTDS pulse trains with a repetition rate of 10 GHz were used as LOs to perform parallel optical sampling.

The wavelengths of the transmitter and the LO laser were 1550 nm and their frequency difference was tuned to be as small as possible. An electroabsorption modulator was modulated by a 10-GHz clock at a proper bias point to achieve a pulse train

Fig. 3. Experimental setup for  $1 \times 2$  COTDS.

with a pulsewidth around 20 ps. The pulse train was then divided into two by a 50-ps relative delay. The two LO pulse trains were adjusted to have orthogonal polarization and then multiplexed by a polarization combiner. The polarization of the received signal is adjusted to be  $45^\circ$  with respect to the two LO pulse trains. In this way, only one  $90^\circ$  optical hybrid is required and the two orthogonal LO pulse trains beat with the received signal independently. The outputs of the hybrid were separated by two polarization splitters and then detected by four detectors with 12-GHz bandwidth. A real-time digital oscilloscope (Agilent DSO80000) was used as ADCs and sampled at 10 Gsa/s. The signal power launched into SSMF was 0 dBm, and the erbium-doped fiber amplifiers had noise figures around 5 dB. The total LO power was set to be  $-2.6$  dBm.

As pointed out in Section II, the phase difference  $\phi_{\text{rel}}$  between the two LO channels should be stable and known to perform EDC and phase estimation properly. In our experiment, we estimated the phase difference in postprocessing. Once  $\phi_{\text{rel}}$  is obtained, it can be compensated since it varies slowly. We chose consecutive “1”s and “0”s, which had small phase change between adjacent sample points even after transmission, to calculate the phase difference between the two LO pulse trains. The corresponding sample points of these consecutive symbols in the two tributaries should have almost the same phase, so they could be used to calculate  $\phi_{\text{rel}}$ . This algorithm was demonstrated for the 220-km SSMF transmission experiment.

After the phase difference estimation, we performed off-line signal processing and bit-error-rate (BER) measurement from recorded data, by applying EDC and phase estimation after transmission. The accumulated dispersion value was 3740 ps/nm. The block size for the phase estimation was 15. A sliding window was used for each symbol in phase estimation [3].

We measured the eye diagram and BER of the 10-Gb/s BPSK signals when the  $1 \times 2$  COTDS was used. For comparison, we also conducted an experiment using a CW LO and 20-Gsa/s ADCs to electronically sample the signals. The eye diagrams before and after EDC and phase estimation of the two schemes are shown in Fig. 4 ( $P_s = -19$  dBm). It can be seen that COTDS worked well for coherent detection and dispersion compensation. The power penalty of using COTDS instead of using double-speed ADC was about 8 dB, 5 dB of which was from power splitting of the signal and the LO, and the rest was mainly attributed to chirp of the LO pulses and low-pass filtering during photodetection. Both penalties (due to chirp and power splitting) are technical and can be eliminated by using unchirped LO pulses and increasing LO power in local oscillator-amplified spontaneous emission (LO-ASE) beat noise limited systems.

The algorithm employed to calculate  $\phi_{\text{rel}}$  for the experimental data requires phase comparison between consecutive samples

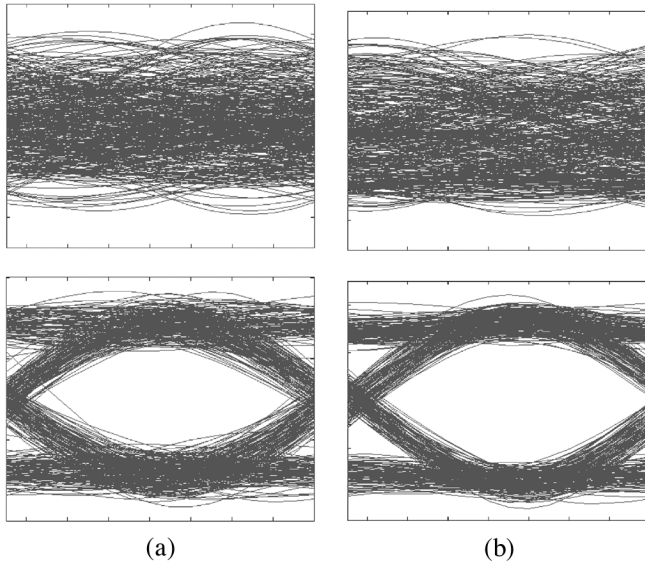


Fig. 4. Eye diagrams before and after dispersion compensation and phase estimation using (a) optical sampling and 10-Gsa/s ADCs and (b) CW LO and 20-Gsa/s ADC. The horizontal scale for all the diagrams is 12.5 ps/div.

from two tributaries and a long data sequence to ensure accurate estimation (4000 samples used in the experiment). A simpler and more practical tracking algorithm can be used to calculate  $\phi_{\text{rel}}$  for real-time implementation. In this case, the data sequence is divided into blocks. Each block is short enough so that  $\phi_{\text{rel}}$  can be treated as a constant within the block. Given  $\phi_{\text{rel}}$  in the previous block, sample points in two tributaries in the present block are chosen if the following condition is met:

$$\left| \phi_{\text{rel}}^{n,i} - \phi_{\text{rel}}^{n-1} \right| \leq \Delta \quad (1)$$

where  $\phi_{\text{rel}}^{n-1}$  is the known phase difference in the previous block,  $\phi_{\text{rel}}^{n,i}$  is the phase difference of the  $i$ th bit in the present block, and  $\Delta$  is the tolerance defined in the algorithm. The phase difference  $\phi_{\text{rel}}$  is then calculated by averaging those qualified sample points. This algorithm was tested by simulation in *VPItransmissionMaker* with a predefined phase difference variation added. The components and settings used in the simulation were the same as those in the experiment. The simulation result is shown in Fig. 5. The phase difference obtained by tracking follows closely the predefined variation, a sinusoid with frequency of 190.73 kHz and peak phase deviation of  $\pm 0.5\pi$ . A block size of 512 bits and a  $\Delta$  value of  $0.3\pi$  were used.

#### IV. CONCLUSION AND DISCUSSION

COTDS was presented to effectively decrease the required PD bandwidth, ADC speed, and DSP rate. Multiple pulse trains were used as LOs and performed coherent optical sampling in parallel. A modified FIR filter for dispersion compensation is needed for parallel implementation. Transmission of 10-Gb/s BPSK signal over 220-km SSMF without optical dispersion compensation was demonstrated using COTDS and 10-Gsa/s

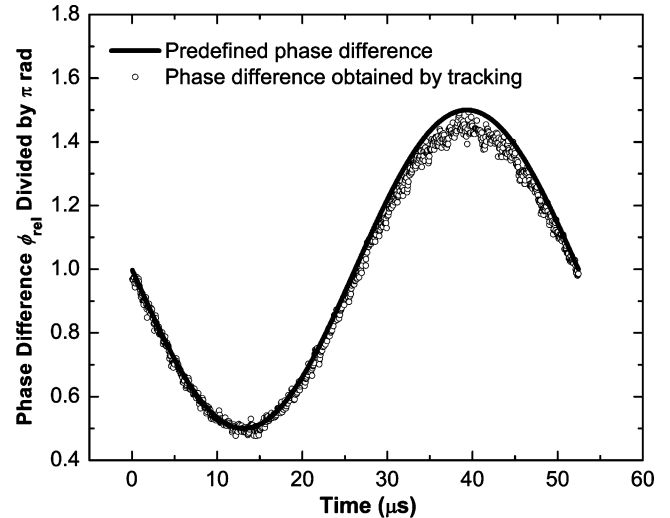


Fig. 5. Estimation of the phase difference between two LOs by tracking algorithm compared with predefined variation.

ADCs. The scheme provides a promising way to coherently detect and process a high-speed optical signal using available low-speed ADCs and DSP units.

In order to maintain coherence between the COTDS LOs, two algorithms for calculating the phase difference were introduced and tested in experiment and in simulation, respectively. It should be noted that the performance of both algorithms depends on data pattern due to fiber dispersion. They work better for long consecutive “1”s and/or “0”s. In the extreme case of a long 101010... pattern, both algorithms would fail. However, the probability of occurrence for this extreme case is statistically small. A combination of two algorithms can be a practical solution to phase difference estimation between the tributaries. By sending the training sequence of consecutive “1”s or “0”s, the initial phase difference can be obtained by the first algorithm. The following tracking can be realized by the second algorithm.

#### REFERENCES

- [1] M. G. Taylor, “Coherent detection method using DSP for demodulation of signal and subsequent equalization of propagation impairments,” *IEEE Photon. Technol. Lett.*, vol. 16, no. 2, pp. 674–676, Feb. 2004.
- [2] S. Tsukamoto, K. Katoh, and K. Kikuchi, “Unrepeated transmission of 20-Gb/s optical quadrature phase-shift-keying signal over 200-km standard single-mode fiber based on digital processing of homodyne-detected signal for group-velocity dispersion compensation,” *IEEE Photon. Technol. Lett.*, vol. 18, no. 9, pp. 1016–1018, May 1, 2006.
- [3] R. Noé, “Phase noise tolerant synchronous QPSK receiver concept with digital I&Q baseband processing,” in *Proc. Opto-Electronics and Communications Conf.*, 2004, pp. 818–819.
- [4] X. Chen, I. Kim, G. Li, H. Zhang, and B. Zhou, “Coherent detection using optical time-domain sampling,” presented at the Optical Fiber Communication Conf. (OFC 2008), San Diego, CA, Feb. 24–28, 2008, Paper JThA62.
- [5] S. L. Woodward, S.-Y. Huang, M. D. Feuer, and M. Boroditsky, “Demonstration of an electronic dispersion compensator in a 100-km 10-Gb/s ring network,” *IEEE Photon. Technol. Lett.*, vol. 15, no. 6, pp. 867–869, Jun. 2003.